NAVY DEPARTMENT
THE DAVID W. TAYLOR MODEL BASIN
WASHINGTON 7, D.C.

INVESTIGATION OF WAVE EFFECTS PRODUCED BY A THIN BODY - TMB MODEL 4125

by

Georg P. Weinblum, Janet J. Kendrick, and
M. Allison Todd

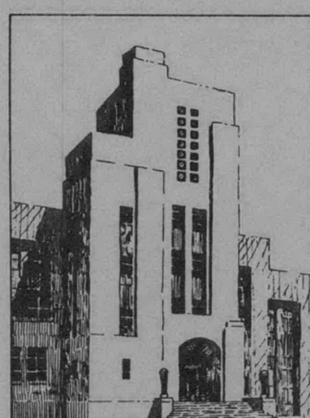

November 1952

Report 840

NOTATION

a	One-half parallel length of model
B	Maximum beam of model
b	One-half maximum beam of model
C_r	Residual resistance coefficient
$C_w = \dfrac{R}{\frac{\rho}{2} Su^2}$	Calculated wave resistance coefficient
F	Froude number
f	Depth of immersion
g	Acceleration due to gravity
H	Draft
H_0	Struve's function
L	Total length of model
l	Parabolic length
M_1	$\int_0^1 \xi \sin \gamma\xi \, d\, \xi$
M_1'	$\int_0^1 \xi \cos \gamma\xi \, d\, \xi$
$p = \dfrac{2a}{L}$	Ratio of parallel length to total length
R	Resistance as calculated from Michell's integral
r	Wave resistance coefficient
S	Wetted surface
u	Velocity
Y_0	Bessel function of the second kind
Z_l	Surface elevation due to symmetrical disturbance
Z_w	Surface elevation due to wave system
α	Waterline coefficient
$\gamma_0 = \dfrac{1}{2F^2}$	
Δ	Displacement
δ	Block coefficient
ζ	Nondimensional vertical measurement

λ	Wave length
ξ	Nondimensional longitudinal measurement
ρ	Density
ϕ	Prismatic coefficient

INVESTIGATION OF WAVE EFFECTS PRODUCED BY A THIN BODY - TMB MODEL 4125

by

Georg P. Weinblum, Janet J. Kendrick, and M. Allison Todd

INTRODUCTION

An opportunity to check experimentally Michell's wave-resistance theory[1] arose when a friction plane or "thin body" was constructed for investigations of the frictional resistance of painted surfaces. In his wave-resistance theory, the only assumption made by Michell as to the form of the ship was that the inclination of the tangent plane at any point of its surface to the vertical median plane should be small.

Although the TMB model is quite narrow, it cannot be considered as a thin plank; thus, appreciable wave effects must be expected when the model is towed at medium and high Froude numbers.

The dimensions of the body are shown in Figure 1. It has a parallel middle body and parabolic ends with vertical sides. Apart from the rectangular form of the sections, this body forms an ideal Michell's ship as defined above due to its very low beam-length ratio [B/L = 0.0265] and beam-draft ratio [B/H = 0.183].

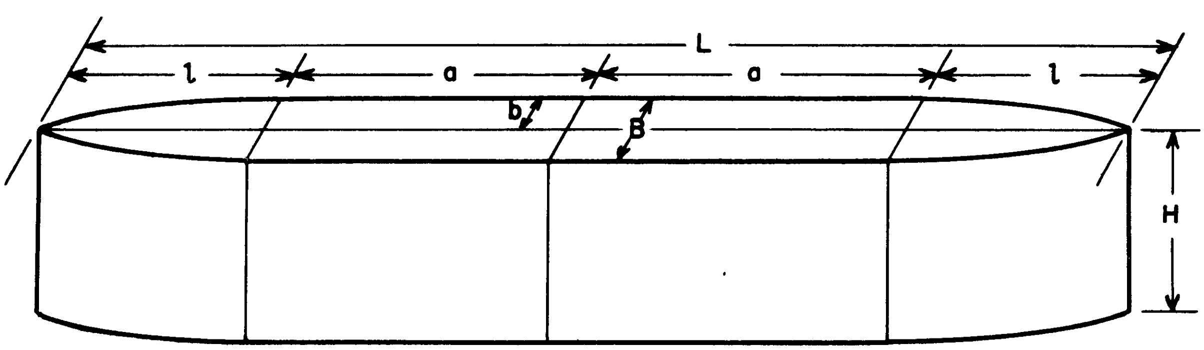

Figure 1 - Shape and Dimensions of Friction Body, TMB Model 4125

L = total length	= 252 inches	H = draft	= 36 inches
l = parabolic length	= 66 inches	a = half parallel length	= 60 inches
B = maximum beam	= 6.69 inches	p = 2a/L	= 0.4762
b = half beam	= 3.345 inches		

---

[1]References are listed on page 14.

It was decided to calculate the wave resistance experienced by the model and the wave profiles along the hull and to compare these theoretical values with the results of experiments.

Auxiliary resistance integrals, which simplify the work considerably, were not available at the time. Since, however, the draft-length ratio H/L is not covered by the systematic computations now being made at the Taylor Model Basin, an independent evaluation was needed in any case and justified the appreciable work involved.

RESISTANCE

The original form of Michell's resistance integral may be reduced to the dimensionless form[2]

$$R = \frac{8\rho g}{\pi} \frac{B^2 H^2}{L} \int_{\gamma_0}^{\infty} \left[I^{*2}(\gamma) + J^{*2}(\gamma) \right] \frac{\left(\frac{\gamma}{\gamma_0}\right)^2}{\sqrt{\left(\frac{\gamma}{\gamma_0}\right)^2 - 1}} d\gamma \qquad [1]$$

$$I^*(\gamma) = \int_0^1 \int_0^1 \frac{\partial \eta_a}{\partial \xi} e^{-2 \frac{H}{L} \frac{\gamma^2}{\gamma_0^2} \zeta} \cos \gamma \, \xi \, d\xi \, d\zeta \qquad [2]$$

$$J^*(\gamma) = \int_0^1 \int_0^1 \frac{\partial \eta_s}{\partial \xi} e^{-2 \frac{H}{L} \frac{\gamma^2}{\gamma_0^2} \zeta} \sin \gamma \, \xi \, d\xi \, d\zeta \qquad [3]$$

where $\xi = \frac{x}{l}$

$\gamma = \gamma_0 \lambda$

$\gamma_0 = \frac{gL}{2v^2} = \frac{1}{2F^2}$

η = waterline equation of hull

$\eta_s = \frac{1}{2}\left[\eta(x) + \eta(-x)\right]$

$\eta_a = \frac{1}{2}\left[\eta(x) - \eta(-x)\right]$

η_s, η_a represent the symmetrical and antisymmetrical parts of the hull with respect to the midship section, and

v = speed of advance.

Since for a symmetrical hull $I^*(\gamma) = 0$, Equation [1] reduces in this case to

$$R = \frac{8\rho g}{\pi} \frac{B^2 H^2}{L} \int_{\gamma_0}^{\infty} \frac{\left(\frac{\gamma}{\gamma_0}\right)^2}{\sqrt{\left(\frac{\gamma}{\gamma_0}\right)^2 - 1}} J^{*2}(\gamma)\, d\gamma \qquad [4]$$

The intermediate function $J^*(\gamma)$ is given in this case by

$$J^*(\gamma) = -2E_0\left[\sin \gamma p M_1' \left\{\gamma(1-p)\right\} + \cos \gamma p M_1 \left\{\gamma(1-p)\right\}\right] \qquad [5]$$

as can be seen by substituting the form of the waterline equation η_s in Equation [3].

Here

$$E_0 = \frac{1-e^{-\vartheta}}{\vartheta} \qquad \vartheta = \frac{2H\gamma^2}{L\gamma_0}$$

$$M_1' = \int_0^1 \xi \cos \gamma \xi \, d\xi$$

$$M_1 = \int_0^1 \xi \sin \gamma \xi \, d\xi$$

Graphs of E_0^2 over ϑ and of $\sin \gamma p M_1' \left\{\gamma(1-p)\right\} + \cos \gamma p M_1 \left\{\gamma(1-p)\right\}$ over γ were plotted; from these the necessary values could be obtained.

The integral was evaluated at the singularity $\gamma/\gamma_0 = 1$ by integrating over a narrow range between $\gamma_0 + \gamma_0(1+\epsilon)$ where $\epsilon \leq 0.01$ using the formula

$$\int_{\gamma_0}^{\gamma_0(1+\epsilon)} \frac{\left(\frac{\gamma}{\gamma_0}\right)^2}{\sqrt{\left(\frac{\gamma}{\gamma_0}\right)^2 - 1}} J^{*2}(\gamma)\, d\gamma = \gamma_0 J^{*2}(\gamma_0)\sqrt{2\epsilon}$$

The main part of the integral

$$\int_{\gamma_0(1+\epsilon)}^{\gamma_1} \frac{\left(\frac{\gamma}{\gamma_0}\right)^2}{\sqrt{\left(\frac{\gamma}{\gamma_0}\right)^2 - 1}} J^{*2}(\gamma)\, d\gamma$$

was evaluated from the graphs of the integrand by means of a planimeter. The remainder

$$\int_{\gamma_1}^{\infty} \frac{\left(\frac{\gamma}{\gamma_0}\right)^2}{\sqrt{\left(\frac{\gamma}{\gamma_0}\right)^2 - 1}} J^{*2}(\gamma)\, d\gamma$$

was calculated from expansion of the integrand.

The resistance was then calculated for two additional drafts, H = 20 inches and 10 inches, and at two Froude numbers for an infinite draft.

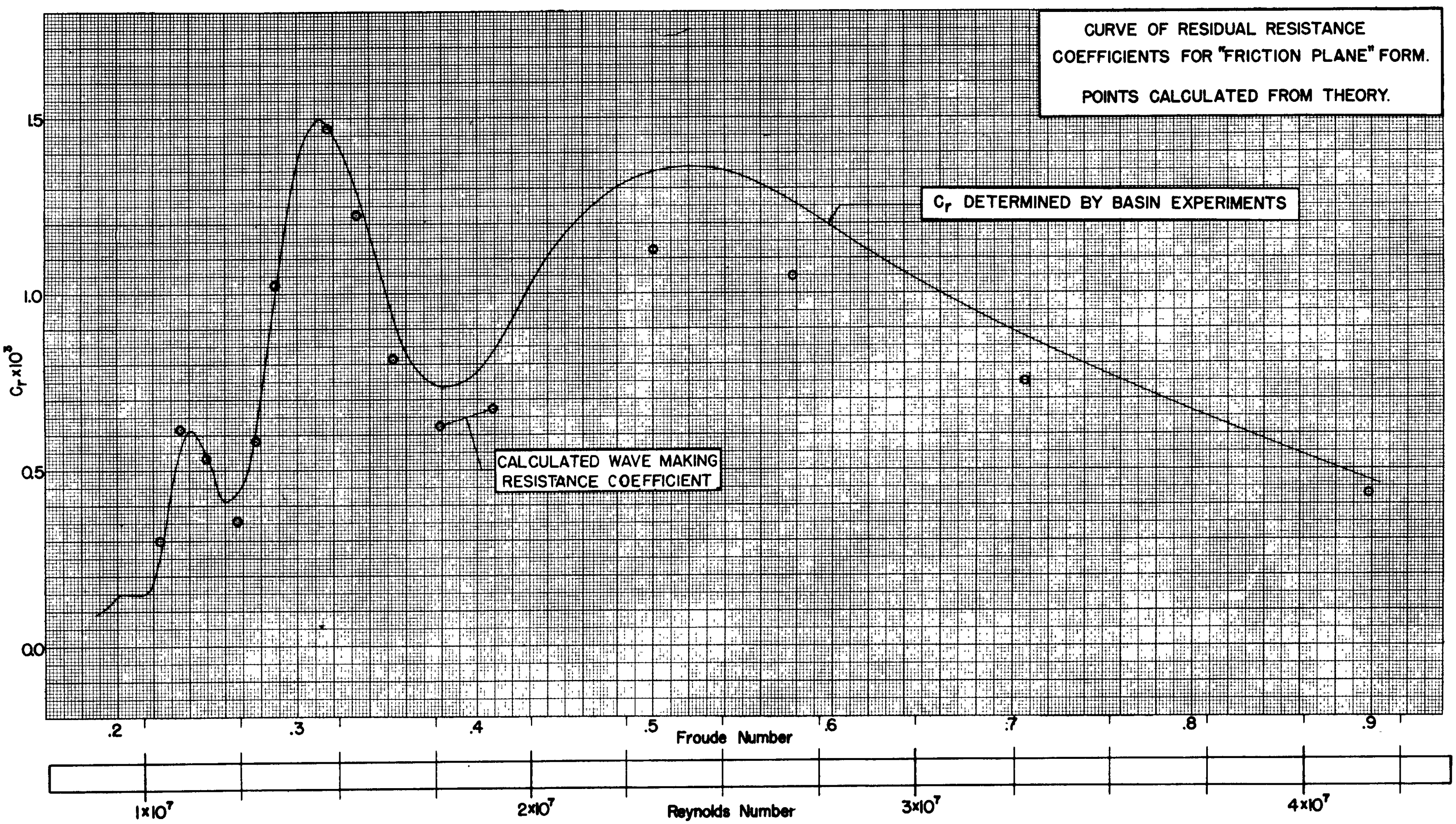

Figure 2 - Comparison of Calculated and Observed Wave Resistance of Model
(Reference 4)

Havelock has given an example showing how to correct resistance data obtained from friction body experiments for the wave resistance.[3] In the discussion of this paper, Weinblum has pointed out that these estimates may be much too low for moderate Froude numbers since they are based on a parabolic waterline while the actual form can be much fuller (see page 269, Reference 3).

The results of the computations are presented in various ways. Figure 2, reproduced from Reference 4, shows the comparison of the calculated wave resistance coefficient $C_w = \dfrac{R}{\frac{\rho}{2} S u^2}$ with the "residual resistance" coefficient C_r. Schoenherr's frictional resistance line was used to evaluate C_w.

The coefficients reach their maximum at moderate Froude numbers which is characteristic of very full forms. Figure 3 shows the calculated wave resistance coefficients $r = \dfrac{R}{\frac{8\rho g}{\pi} \frac{B^2 H^2}{L}}$ plotted against $\gamma_0 = \dfrac{1}{2F^2}$ for three depth-length ratios.

Figure 4 shows the wave resistance coefficients of a parabolic form (for which $p = 0$) with the same proportions as the friction body. It can be seen that for this form, the coefficient of resistance is much lower than that of the fuller form except in the region of the large hump.

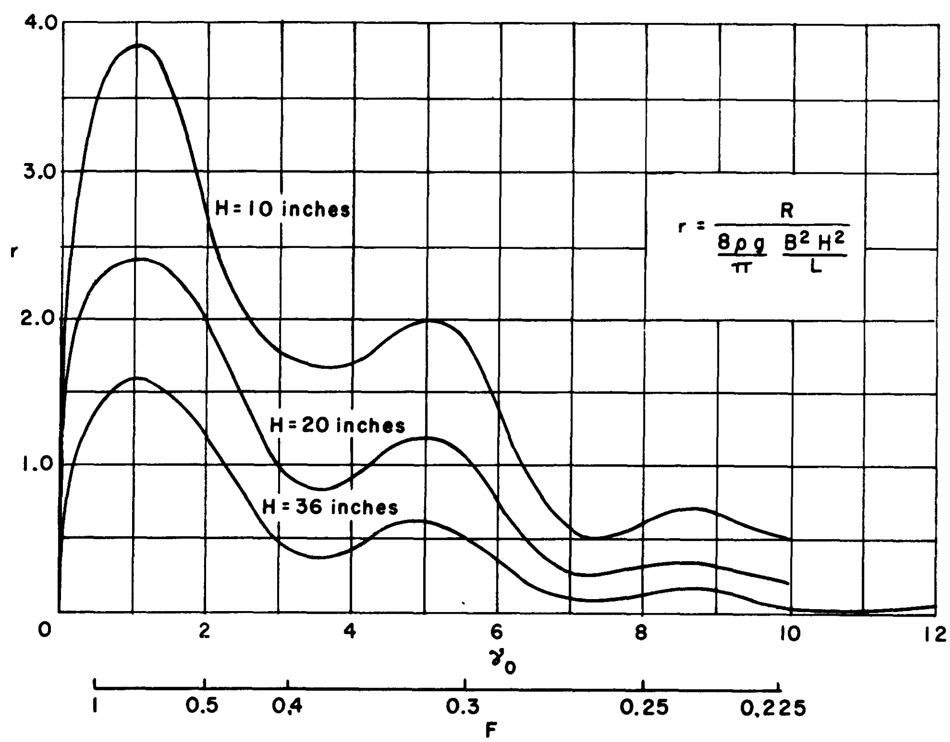

Figure 3 - Wave Resistance Coefficients r Plotted Against Speed for Three Different Drafts

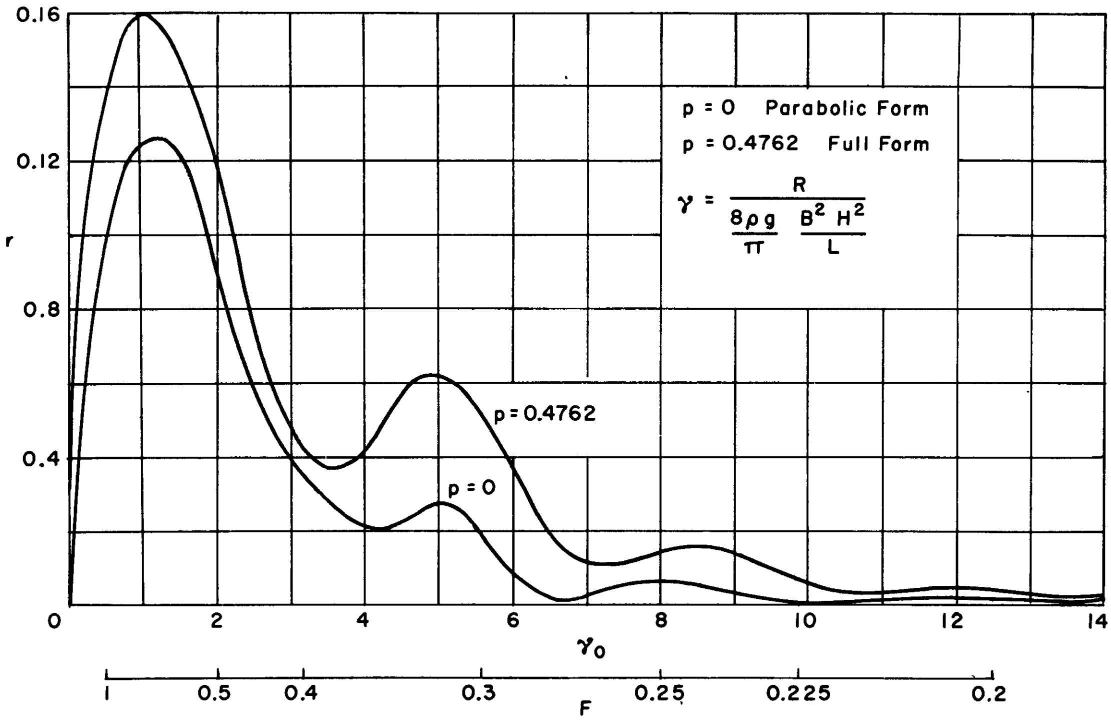

Figure 4 - Comparison of Wave Resistance Coefficients of Parabolic and Full Forms

To obtain a better basis of comparison between theory and experiment, it was suggested that the influence of the sharp corners on the resistance should be eliminated by towing the model at a shallower draft $H = 20$ inches. Then the measured and calculated differences in resistance for the two drafts could have been calculated. However, it was not feasible to tow the model at a shallower draft at the time the tests were run.

WAVE PROFILES

The work done on the calculation of the wave profiles of the friction body was based upon information given by W.C.S. Wigley.[5] His investigations were performed upon a body having a short parallel middle body, 1/16 of the total length, and parabolic ends.

Since the subject of wave profiles has not been treated as frequently as that of wave resistance, the computations are presented here in detail.

Two formulas given by Wigley in dimensional form were used in the calculations of the wave profiles. The first gave the surface elevation due to wave making and the second the symmetrical disturbance.

In dimensionless coefficients these become

$$\frac{\pi\gamma(1-p)Z_w}{8b} = P_0\left\{\gamma\xi\right\} + P_0\left\{\gamma(\xi-2)\right\} - \frac{1}{\gamma(1-p)}\Big[P_0^{-1}\left\{\gamma\xi\right\} - P_0^{-1}\left\{\gamma(\xi-1+p)\right\} - P_0^{-1}\left\{\gamma(\xi-2)\right\} + P_0^{-1}\left\{\gamma(\xi-1-p)\right\}\Big] \qquad [6]$$

and

$$\frac{\pi\gamma(1-p)Z_l}{2b} = -\left[Q_0\left\{\gamma\xi\right\} + Q_0\left\{\gamma(\xi-2)\right\} - \frac{1}{\gamma(1-p)}\left(Q_1\left\{\gamma\xi\right\} - Q_1\left\{\gamma(\xi-1+p)\right\} + Q_1\left\{\gamma(\xi-1-p)\right\} - Q_1\left\{\gamma(\xi-2)\right\}\right)\right] \quad [7]$$

where Z_l is the surface elevation due to non-wave portion of disturbance caused by motion of the form,* and Z_w is the surface elevation due to wave system.

The nondimensional longitudinal distance ξ is positive when measured in the astern direction. The basic functions P and Q are defined as follows:[7, 8]

$$P_0(u) = \int_0^{\frac{\pi}{2}} \sin(u \sec\phi)\, d\phi$$

$$P_0^{-1}(u) = 1 + P_1(u) = 1 - \int_0^{\frac{\pi}{2}} \cos\phi \cos(u\sec\phi)\, d\phi$$

In the present calculations, the values of the P functions were obtained from a graph prepared by Professor Lunde.[7]

$$Q_0(u) = \frac{\pi}{2}\int_0^u \left\{H_0(t) - Y_0(t)\right\} dt$$

where $H_0(t)$ is Struve's function and $Y_0(t)$ is the Bessel function of the second kind. The values of $Q_0(u)$ may be calculated for values of $t \le 16$ using the tables of $H_0(t)$ and $Y_0(t)$ given by Watson.[9] For values of $t > 16$ (for which the values of $H_0(t)$ and $Y_0(t)$ are not given), the following method was used:

When t is large (in this case for $t > 16$)

$$H_0(t) = Y_0(t) + \frac{1}{\pi}\sum_{m=0}^{m} \frac{\Gamma\left(m+\frac{1}{2}\right)}{\Gamma\left(\frac{1}{2}-m\right)\left(\frac{1}{2}t\right)^{2m+1}} .$$

Therefore

$$Q_0(t) - Q_0(16) = \frac{1}{2}\int_{16}^{u} \sum_{m=0}^{m} \frac{\Gamma\left(m+\frac{1}{2}\right)}{\Gamma\left(\frac{1}{2}-m\right)\left(\frac{1}{2}t\right)^{2m+1}}\, dt$$

*"The function Q_0 does not oscillate but is monotonic, and the terms in Q_0 represent a symmetrical disturbance of the surface in the neighborhood of the form which dies away quickly both fore and aft of the form. It absorbs no energy owing to its symmetry and therefore does not affect the resistance."[6]

TABLE 1

Values for $Q_0(u) = \frac{\pi}{2}\int_0^u [H_0(t) - Y_0(t)]\, dt$.

u	$Q_0(u)$	u	$Q_0(u)$	u	$Q_0(u)$
0	0	9.5	3.538	20.5	4.303
0.2	0.563	10.0	3.589	21.0	4.327
0.4	0.880	10.5	3.637	21.5	4.350
0.6	1.118	11.0	3.681	22.0	4.373
0.8	1.311	11.5	3.727	22.5	4.396
1.0	1.474	12.0	3.770	23.0	4.418
1.5	1.801	12.5	3.810	23.5	4.439
2.0	2.051	13.0	3.849	24.0	4.460
2.5	2.244	13.5	3.887	24.5	4.481
3.0	2.420	14.0	3.923	25.0	4.501
3.5	2.565	14.5	3.958	25.5	4.521
4.0	2.693	15.0	3.991	26.0	4.540
4.5	2.806	15.5	4.024	26.5	4.559
5.0	2.908	16.0	4.056	27.0	4.578
5.5	3.000	16.5	4.087	27.5	4.596
6.0	3.085	17.0	4.116	28.0	4.614
6.5	3.164	17.5	4.145	28.5	4.632
7.0	3.237	18.0	4.173	29.0	4.649
7.5	3.333	18.5	4.201	29.5	4.666
8.0	3.368	19.0	4.227	30.0	4.683
8.5	3.428	19.5	4.253		
9.0	3.485	20.0	4.278		

TABLE 2

Values for $Q_1(u) = \int_0^u Q_0(t)\,dt$

u	$Q_1(u)$	u	$Q_1(u)$	u	$Q_1(u)$
0	0	9.5	24.988	20.5	68.636
0.2	0.065	10.0	26.775	21.0	70.803
0.4	0.209	10.5	28.577	21.5	72.963
0.6	0.412	11.0	30.411	22.0	75.153
0.8	0.653	11.5	32.258	22.5	77.336
1.0	0.933	12.0	34.138	23.0	79.549
1.5	1.755	12.5	36.028	23.5	81.753
2.0	2.718	13.0	37.947	24.0	83.988
2.5	3.796	13.5	39.877	24.5	86.213
3.0	4.959	14.0	41.834	25.0	88.468
3.5	6.211	14.5	43.799	25.5	90.714
4.0	7.521	15.0	45.791	26.0	92.989
4.5	8.902	15.5	47.791	26.5	95.254
5.0	10.325	16.0	49.815	27.0	97.548
5.5	11.808	16.5	51.846	27.5	99.832
6.0	13.324	17.0	53.902	28.0	102.144
6.5	14.892	17.5	55.958	28.5	104.446
7.0	16.487	18.0	58.047	29.0	106.776
7.5	18.132	18.5	60.131	29.5	109.095
8.0	19.810	19.0	62.247	30.0	111.442
8.5	21.504	19.5	64.358		
9.0	23.237	20.0	66.500		

Evaluating to the first two terms only

$$Q_0(t) - Q_0(16) = \frac{1}{2}\int_{16}^{u}\left[\frac{\sqrt{\pi}}{\sqrt{\pi}\,\frac{t}{2}} + \frac{\frac{1}{2}\sqrt{\pi}}{-2\sqrt{\pi}\,\frac{t^3}{8}}\right]dt$$

$$= \frac{1}{2}\int_{16}^{u}\left(\frac{2}{t} - \frac{2}{t^3}\right)dt \qquad [8]$$

$$= \log t + \frac{1}{2t^2} - \log 16 - \frac{1}{512}$$

$Q_0(u)$ was evaluated for $16 < t \le 30$ using Equation [8]. A tabulation of these values is given in Table 1.

The values of $Q_1(u) = \int_0^u Q_0(t)\,dt$ were obtained from these by integration; see Table 2.

The P-functions are not defined for negative values of t. $P(-|t|) = 0$ was used. Thus, it can be seen from Equation [6] for Z_w that for $0 \le \xi \le 1 - p$ only the terms $P_0(\gamma\xi)$ and $P_0^{-1}(\gamma\xi)$ are defined. For $1 - p \le \xi \le 1 + p$ the term $P_0^{-1}\{\gamma(\xi - \overline{1 - p})\}$ is defined. For $1 + p \le \xi \le 2$ the term $P_0^{-1}\{\gamma(\xi - \overline{1 + p})\}$ is also defined and for $\xi \ge 2$ all are defined. It would appear then that the first two terms mentioned would give the ordinates of the bow wave system, the next the ordinates for the waves proceeding from the foreshoulder, the fourth the ordinates of the waves proceeding from the aftershoulder, and the last two the ordinates of the stern wave system.

In the example given in the present paper (Figure 6), these four waves are plotted separately to show the components of the total wave system contributed by each of the terms considered above.

The Q-functions appearing in the equation for the symmetrical disturbance[7] are defined for negative values of t as:

$$Q_0(-t) = Q_0(t) \qquad \text{and} \qquad Q_1(-t) = -Q_1(t)$$

Thus all the terms of Equation [7] are defined for all values of ξ.

The evaluation of Equations [6] and [7] give the wave profiles in terms of dimensionless coefficients containing Z_w and Z_l. The multiplication of these values by the constants $\frac{8b}{\pi\gamma(1-p)}$ and $\frac{2b}{\pi\gamma(1-p)}$ respectively, transforms them into the dimensions of b. In Figure 7 the calculated and observed profiles are plotted to an inch scale. In Figure 6, however, the components are plotted in dimensionless form.

The comparison was made as outlined above for five different speeds. At the lower speeds (4.5 and 5 knots) the agreement between the observed and calculated profiles is good; for higher speeds the agreement of the crests is good but the troughs of the calculated profiles are deeper than those observed (Figure 7). This is at least partly accounted for by the assumption of infinite draft made throughout the calculation. The influence of a finite draft will be more marked at higher speeds. This will be evident from a consideration of the

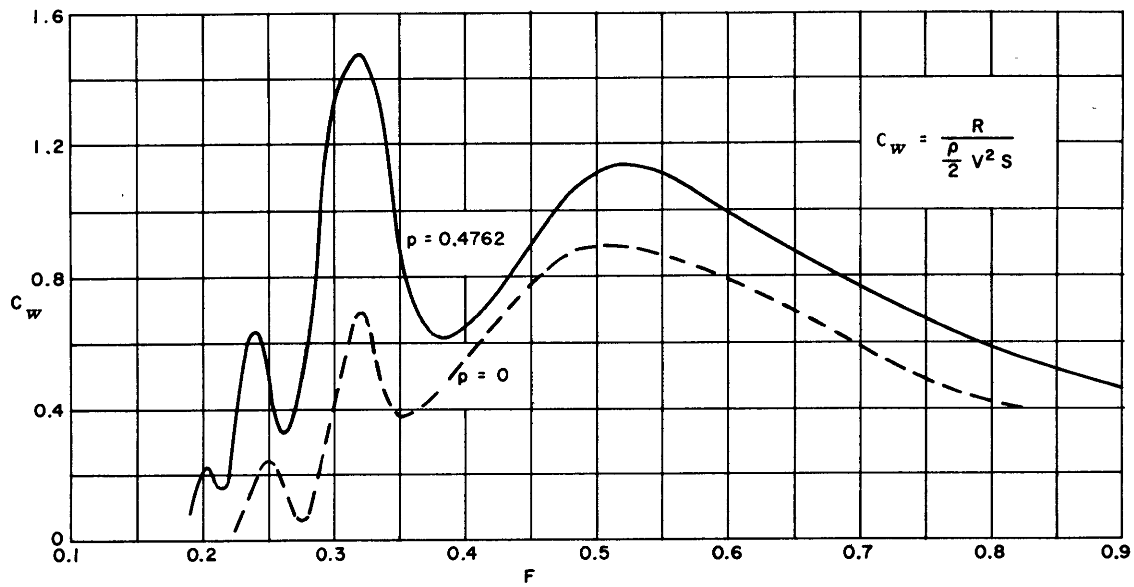

Figure 5 - Wave Resistance Coefficient C_w Plotted Against Froude Number for Parabolic and Full Forms

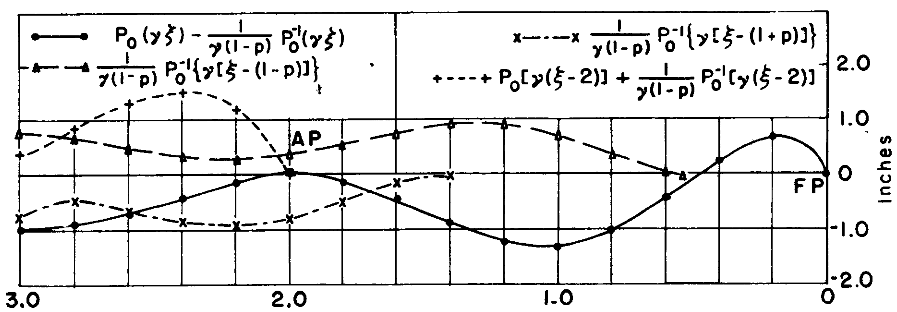

Figure 6a - Main Surface Elevation

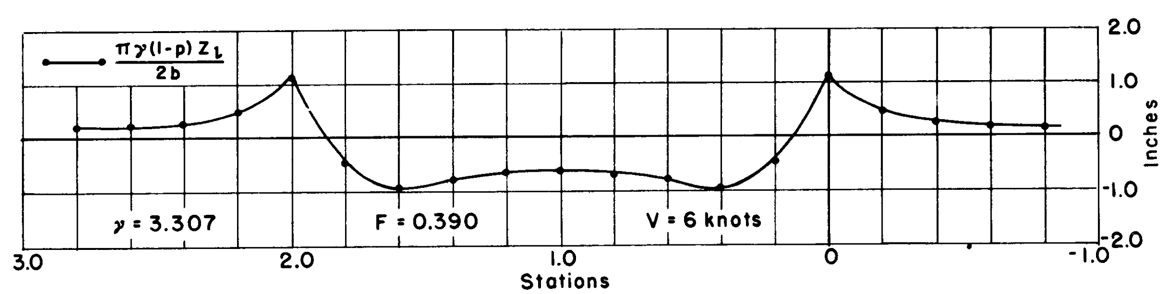

Figure 6b - Symmetrical Disturbance

Figure 6 - Wave Profiles for Speed of Advance of 6 Knots Plotted in Dimensionless Coefficients and Showing Components

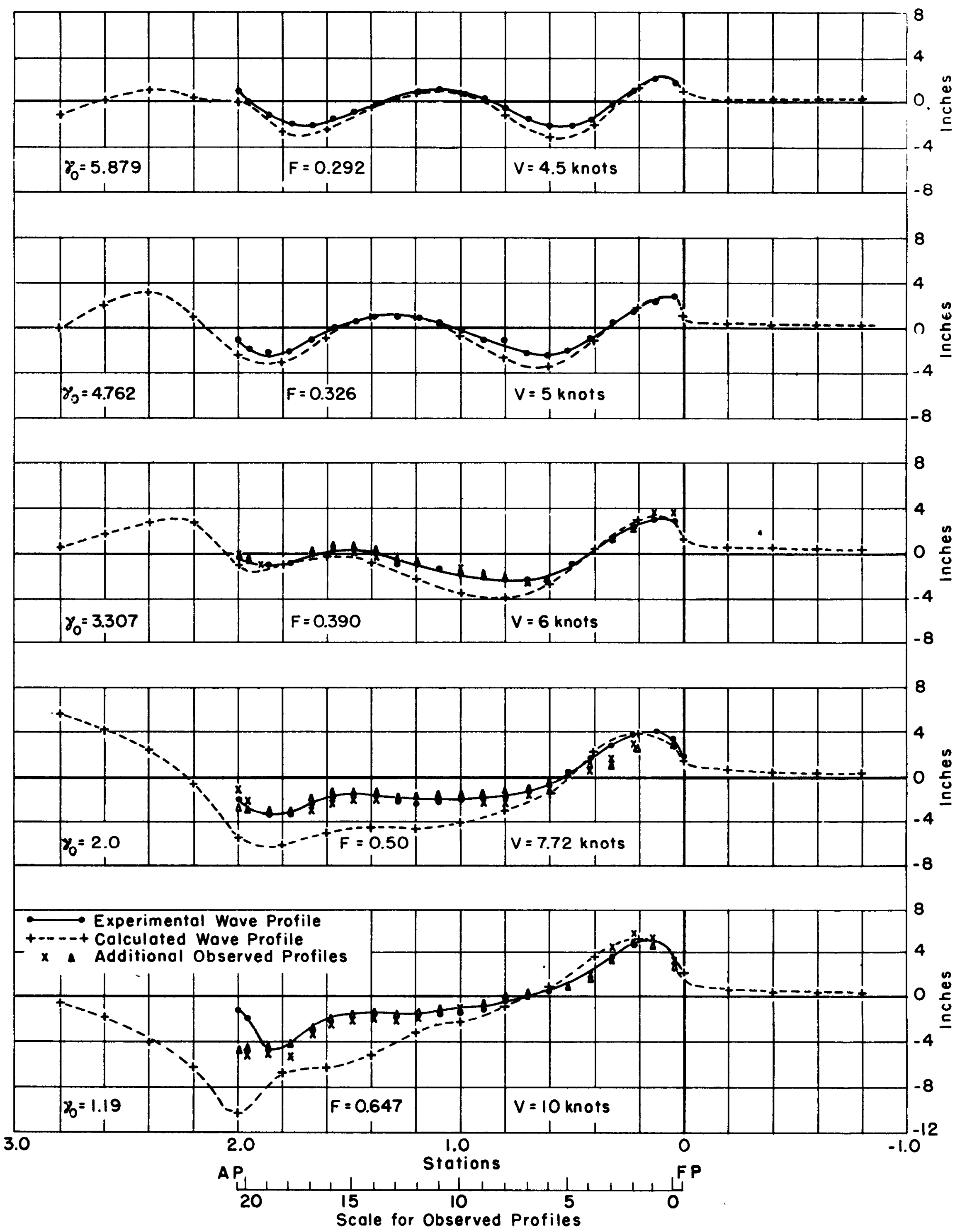

Figure 7 - Comparison of Calculated and Measured Wave Profiles for Five Different Speeds of Advance

exponential term relating the below-surface disturbing pressures to the wave length at the surface and the depth of immersion. These forces vary approximately as $e^{-\frac{2\pi f}{\lambda}}$ where f is the depth of immersion and λ is the wave length. Thus as λ increases with increasing speed, $e^{-\frac{2\pi f}{\lambda}}$ also increases. The effect upon the water surface elevation of the finite draft of the model will, therefore, be greater at higher speeds than at low, and better agreement than that actually obtained cannot be expected.

It was found that measuring the wave profile at the bow sometimes presents serious difficulties because of the steep slope of the wave in a transverse plane. Photographs of wave contours along the ship may therefore prove to be rather unreliable.

CONCLUSION

The qualitative and quantitative agreements between the calculated wave resistance coefficient C_w and the residual resistance coefficient C_r (as shown in Figure 2) are very satisfactory. In particular, prediction of the "third" hump* was possible in the resistance curve of Figure 3 at $F = 0.24$ which at first escaped the attention of the experimenters.

Because of this good agreement, the following deductions from the computations can be relied upon without further checks:

It is well known that because of the linear character of Michell's analysis the relation $R \sim B^2$ holds.

It can also be demonstrated that at very large Froude numbers ($\gamma \to 0$) the integral r becomes independent of H/L provided this ratio is finite. Thus the three curves on Figure 3 must finally coincide and $R \sim B^2H^2$, i.e., the wave resistance in this range is proportional also to the square of the depth H. However, it can be seen from the figures that this asymptotic relation does not hold for high-speed displacement ships. For example, at a destroyer speed of $F = 0.6$, $\gamma = 1.5$. In this case R is proportional to $H^{1.5}$ only; at $F = 0.25$, $R \sim H^2$ where r is already less than unity.

The studies of the method of formation of wave systems described in this report explain to some extent the characteristic form of the wave-resistance curve.

It can readily be seen that with increasing speed and therefore with increasing wave length, the crests of the bow wave system will alternately reinforce and dampen those of the stern and shoulder wave systems. Similarly, combinations of these systems will change with changing speed. These reinforcing and damping effects of the wave systems account for the

*The hump in the resistance coefficient curve occurring at $F \cong 0.5$ is here denoted as the "first" hump, at $F \cong 0.3$ as the "second" hump, etc. (see Figure 3), contrary to the custom in naval architecture by which the hump at the highest speed is called the last hump. This change appeared to be necessary since from a mathematical viewpoint there are an infinite number of humps between $0.5 \geq F \geq 0$ (see also Reference 2, page 23).

peaks and hollows seen in the curve of wave resistance plotted against speed. However, after a certain speed is reached, even the second wave of the bow wave system will be astern of the ship, and there can be no further reinforcement of the other systems. Above this speed, therefore, the wave resistance curve will have no further peaks but will show a steady fall with further increase in speed.

ACKNOWLEDGMENT

The authors with to express their thanks to the Surface Ship Powering Section for the experimental contributions utilized in this report.

REFERENCES

1. Michell, J.H., "The Wave Resistance of a Ship," The London Edinburgh and Dublin Philosophical Magazine and Journal of Science, January-June 1898.

2. Weinblum, G.P., "Analysis of Wave Resistance," TMB Report 710, September 1950, p. 91.

3. Havelock, T.H., "Calculations Illustrating the Effect of Boundary Layer on Wave Resistance," Transactions of the Institute of Naval Architects, Vol. 90, 1948.

4. Couch, R.B., "Preliminary Report of Friction Plane Resistance Tests of Antifouling Ship-Bottom Paints," TMB Report 789, August 1951.

5. Wigley, W.C.S., "A Comparison of Experiment and Calculated Wave Profiles and Wave Resistance of a Form Having Parabolic Waterlines," Proceedings of the Royal Society, Series A, Vol. 144, 1934.

6. Wigley, W.C.S., "Ship Wave Resistance: An Examination and Comparison of the Speeds of Maximum and Minimum Resistance in Practice and in Theory," Northeast Coast Institution, 13 February 1931.

7. Lunde, J.K., Unpublished work sent to Dr. Weinblum in letter of 13 January 1949.

8. Havelock, T.H., "Studies in Wave Resistance, Influence of the Form of the Water Plane Section of the Ship," Proceedings of the Royal Society, Series A, Vol. 103, 1923.

9. Watson, G.N., "A Treatise on the Theory of Bessel Functions," The Macmillan Company, New York, 1944.

INITIAL DISTRIBUTION

Copies	
16	Chief, Bureau of Ships, Technical Library (Code 327), for distribution: 5 Technical Library 1 Deputy and Assistant to Chief (Code 101) 1 Technical Assistant to Chief (Code 106) 1 Research (Code 300) 1 Applied Science (Code 370) 1 Ship Design (Code 410) 2 Preliminary Design (Code 420) 1 Submarines (Code 515) 1 Minesweeping (Code 520) 1 Torpedo Countermeasures (Code 520c) 1 Sonar (Code 940)
4	Chief of Naval Research, for distribution: 3 Fluid Mechanics (N426) 1 Undersea Warfare (466)
1	Chief, Bureau of Aeronautics, Aero and Hydrodynamics (DE-3)
2	Chief, Bureau of Ordnance, Underwater Ordnance (Re6a), Attn: Dr. Maxfield
2	Chief, Bureau of Ordnance, Re3, Attn: Dr. Miller
1	Commander, Submarine Force, U.S. Atlantic Fleet
1	Commander, Submarine Force, U.S. Pacific Fleet
1	Commander, Portsmouth Naval Shipyard, Portsmouth, N.H.
1	Commander, Mare Island Naval Shipyard, Vallejo, Calif.
2	Commander, U.S. Naval Ordnance Laboratory, White Oaks, Silver Spring 19, Md.
1	Director, U.S. Naval Research Laboratory, Washington 25, D.C.
2	Commander, U.S. Naval Ordnance Test Station, Underwater Ordnance Division, Pasadena, Calif.
1	Commanding Officer and Director, U.S. Navy Underwater Sound Laboratory, Fort Trumbull, New London, Conn.
1	Commanding Officer and Director, U.S. Navy Electronics Laboratory, San Diego 52, Calif.
1	Commanding Officer, U.S. Naval Underwater Ordnance Station, Newport, R.I.
1	Executive Secretary, Research and Development Board, Pentagon, Washington 25, D.C.
1	Commanding Officer, U.S. Naval Administrative Unit, Massachusetts Institute of Technology, Cambridge 39, Mass.
1	Director, Office of Naval Research Branch Office, 150 Causeway Street, Boston 10, Mass.

Copies

Copies	
1	Director, Office of Naval Research Branch Office, 346 Broadway, New York 13, N.Y.
1	Director, Office of Naval Research Branch Office, America Fore Bldg., 844 N. Rush Street, Chicago 11, Ill.
1	Director, Office of Naval Research Branch Office, 1000 Geary Street, San Francisco 9, Calif.
1	Director, Office of Naval Research Branch Office, 1030 East Green Street, Pasadena 1, Calif.
2	Officer in Charge, Office of Naval Research Branch Office, London, England, Navy 100, FPO, New York, N.Y.
6	Director of Aeronautical Research, National Advisory Committee for Aeronautics, 1724 F Street, N.W., Washington 25, D.C.
2	Director, Experimental Towing Tank, Stevens Institute of Technology, 711 Hudson Street, Hoboken, N.J.
1	Director, Technical Information Branch, Aberdeen Proving Ground, Aberdeen, Md.
2	RADM A.I. McKee, USN (Ret.), Member, Panel on the Hydrodynamics of Submerged Bodies and Asst. General Manager, General Dynamics Corp., Electric Boat Division, Groton, Conn.
1	Dr. G.F. Wislicenus, Member, Panel on the Hydrodynamics of Submerged Bodies and Chairman, Department of Mechanical Engineering, Johns Hopkins University, Baltimore, Md.
1	RADM P.F. Lee, USN (Ret.), Member, Panel on the Hydrodynamics of Submerged Bodies and Vice President, Gibbs and Cox, Inc., New York, N.Y.
1	Mr. F.L. Thompson, Member, Panel on the Hydrodynamics of Submerged Bodies and Director of Research, Langley Aeronautical Laboratory, Langley Air Force Base, Va.
1	Captain W.S. Diehl, USN, Associate Member, Panel on the Hydrodynamics of of Submerged Bodies, Bureau of Aeronautics, Navy Department, Washington, D.C.
2	Newport News Shipbuilding and Dry Dock Co., Newport News, Va., for distribution: 1 Senior Naval Architect 1 Supervisor, Hydraulics Laboratory
1	Director, Woods Hole Oceanographic Institution, Woods Hole, Mass.
2	Hydrodynamics Laboratory Attn: Executive Committee, California Institute of Technology, 1201 E. California Street, Pasadena 4, Calif.
1	Director, Ordnance Research Laboratory, Pennsylvania State College, State College, Pa.
1	Mr. W. Vermeulen, General Electric Co., Schenectady, N.Y.

Copies	
1	Dr. J.M. Robertson, Chairman, BuOrd Hydroballistics Advisory Committee, c/o Ordnance Research Laboratory, Pennsylvania State College, State College, Pa.
1	Mr. J.P. Breslin, Gibbs and Cox, Inc., 21 West Street, New York 6, N.Y.
1	Dr. C. Kaplan, Langley Aeronautical Laboratory, Langley Air Force Base, Va.
1	Dr. Hunter Rouse, Director, Iowa Institute of Hydraulic Research, State University of Iowa, Iowa City, Iowa
1	Dr. L.G. Straub, Director, St. Anthony Falls Hydraulic Laboratory, University of Minnesota, Minneapolis 14, Minn.
1	Prof. L.A. Baier, Director, Experimental Naval Tank, Department of Naval Architecture and Marine Engineering, University of Michigan, Ann Arbor, Mich.
1	Dr. V.L. Streeter, Illinois Institute of Technology, 3300 Federal Street, Chicago 16, Ill.
2	Dr. George C. Manning, Head, Department of Naval Architecture and Marine Engineering, Massachusetts Institute of Technology, Cambridge 39, Mass.
1	Dr. C.C. Lin, Department of Mathematics, Massachusetts Institute of Technology, Cambridge 39, Mass.
1	Director, Applied Physics Laboratory, Johns Hopkins University, 8621 Georgia Avenue, Silver Spring, Md.
1	Prof. W.S. Hamilton, Technological Institute, Northwestern University, Evanston, Ill.
1	Prof. Garrett Birkhoff, Harvard University, Cambridge 38, Mass.
1	Prof. W. Spannhake, Armour Research Foundation, 35 West 33rd Street, Chicago 16, Ill.
1	Dr. J.V. Wehausen, Editor, Mathematical Reviews, Brown University, Providence 12, R.I.
1	Department of Civil Engineering, Colorado A and M College, Fort Collins, Colo.
1	Dr. D. Gilbarg, Department of Mathematics, Indiana University, Bloomington, Ind.
1	Prof. J. Vennard, Department of Civil Engineering, Stanford University, Stanford, Calif.
1	Director, U.S. Waterways Experiment Station, Vicksburg, Miss.
1	Dr. Garbis H. Keulegan, National Bureau of Standards, Washington, D.C.
2	Director, Institute for Fluid Dynamics and Applied Mathematics, University of Maryland, College Park, Md., one for Dr. Weinstein, one for Physics Department
1	Dr. K.E. Schoenherr, School of Engineering, University of Notre Dame, Notre Dame, Ind.

Copies	
1	Prof. R.A. Dodge, Engineering Mechanics Department, University of Michigan, Ann Arbor, Mich.
1	Dr. A.T. Ippen, Director, Hydrodynamics Laboratory, Department of Civil and Sanitary Engineering, Massachusetts Institute of Technology, Cambridge 39, Mass.
1	Prof. J.L. Hooper, Alden Hydraulic Laboratory, Worcester Polytechnic Institute, Worcester, Mass.
1	Dr. Th. von Kármán, 1051 South Marengo Street, Pasadena, Calif.
1	Dr. M.S. Plesset, California Institute of Technology, Pasadena 4, Calif.
1	Dr. A.G. Strandhagen, School of Engineering, University of Notre Dame, Notre Dame, Ind.
1	Dr. V.L. Schiff, Stanford University, Stanford, Calif.
1	Director, Institute for Mathematics and Mechanics, New York University, 45 Fourth Avenue, New York 3, N.Y.
1	Director, Institute of Aeronautical Sciences, 2 East 64th Street, New York 21, N.Y.
1	Head, Aeronautical Engineering Department, Catholic University, Washington, D.C.
1	Chairman, Department of Aeronautical Engineering, New York University, University Heights, New York 53, N.Y.
1	Administrator, Webb Institute of Naval Architecture, Crescent Beach Road, Glen Cove, Long Island, N.Y.
1	Prof. M.H. Martin, Head of Mathematics Department, University of Maryland, College Park, Md.
1	Librarian, American Society of Mechanical Engineers, 29 West 39th Street, New York 18, N.Y.
1	Librarian, American Society of Civil Engineers, 33 West 39th Street, New York 18, N.Y.
1	Librarian, Daniel Guggenheim Aeronautical Laboratory, California Institute of Technology, Pasadena 4, Calif.
1	Librarian, Carnegie Institute of Technology, Pittsburgh 13, Pa.
1	Librarian, College of Engineering, Cornell University, Ithaca, N.Y.
1	Librarian, Illinois Institute of Technology, 3300 Federal Street, Chicago 16, Ill.
1	Librarian, Rensselear Polytechnic Institute, Troy, N.Y.
1	Librarian, Franklin Institute, Parkway at 20th Street, Philadelphia, Pa.
1	Librarian, Stanford University Libraries, Stanford, Calif.

Copies	
1	Librarian, University of Pennsylvania, Philadelphia 4, Pa.
1	Librarian, Pacific Aeronautical Library, Institute of the Aeronautical Sciences, 7660 Beverly Blvd., Los Angeles 36, Calif.
1	Editor, Aeronautical Engineering Review, 2 East 64th Street, New York 21, N.Y.
1	Editor, Bibliography of Technical Reports, Office of Technical Services, U.S. Department of Commerce, Washington 25, D.C.
1	Captain R. Brard, Directeur, Bassin d'Essais des Carenes, 6 Boulevard Victor, Paris (15e), France
1	Dr. F. Ursell, Trinity College, Cambridge, England
1	Prof. J.K. Lunde, Skipsmodelltanken, Tyholt, Trondheim, Norway
1	Prof. L. Troost, Superintendent, Netherlands Ship Model Basin, Haagsteeg 2, Wageningen, The Netherlands
1	Prof. H. Nordstrom, Director, Swedish State Shipbuilding Experimental Tank, Göteborg 24, Sweden
1	Dr. S.L. Smith, Director, British Shipbuilding Research Association, 5, Chesterfield Gardens, Curzon Street, London W.1, England
1	Dr. L. Malavard, Office, National d'Etudes et de Recherches Aéronautiques, 25 Avenue de la Division - Le Clerc, Chatillon, Paris, France
1	Dr. J.F. Allan, Superintendent, Ship Division, National Physical Laboratory, Teddington, Middlesex, England
1	Dr. J. Dieudonné, Directeur, Institute de Recherches de la Construction Navale, 1 Boulevard Haussmann, Paris (9e), France
1	Dr. G.P. Weinblum, Edmund Siemens Allee 1, Universitaet, Hamburg, Germany
1	Prof. T.H. Havelock, 8 Westfield Drive, Gosforth, Newcastle-on-Tyne, 3, England
1	Mr. C. Wigley, 6-9 Charterhouse Square, London EC-1, England
1	Gen. Ing. U. Pugliese, Presidente, Istituto Nazionale per Studi ed Esperienze di Architettura Navale, Via della Vasca Navale 89, Rome, Italy
1	Sr. M. Acevedo y Campoamor, Director, Canal de Experienceas Hidrodinamicas, El Pardo, Madrid, Spain
1	Head, Aerodynamics Department, Royal Aircraft Establishment, Farnborough, Middlesex, England
1	Director, Hydrodynamics Laboratory, National Research Council, Ottawa, Canada
9	British Joint Services Mission (Navy Staff), P.O. Box 165, Benjamin Franklin Station, Washington, D.C.

David W. Taylor Model Basin. Rept. 840.
INVESTIGATION OF WAVE EFFECTS PRODUCED BY A THIN BODY - TMB MODEL 4125, by Georg P. Weinblum, Janet J. Kendrick, and M. Allison Todd. Washington, November 1952. ii, 14 p. incl. tables, figs., refs.
UNCLASSIFIED

A thin friction body is used to check experimentally Michell's wave resistance theory. The wave resistance experienced by the model and the wave profiles along the hull are calculated. These theoretical values are compared with the results of the experiments.

1. Waves
I. Weinblum, Georg P.
II. Kendrick, Janet J., jt. auth.
III. Todd, M. Allison, jt. auth.
IV. Title: Wave effects produced by a thin body

David W. Taylor Model Basin. Rept. 840.
INVESTIGATION OF WAVE EFFECTS PRODUCED BY A THIN BODY - TMB MODEL 4125, by Georg P. Weinblum, Janet J. Kendrick, and M. Allison Todd. Washington, November 1952. ii, 14 p. incl. tables, figs., refs.
UNCLASSIFIED

A thin friction body is used to check experimentally Michell's wave resistance theory. The wave resistance experienced by the model and the wave profiles along the hull are calculated. These theoretical values are compared with the results of the experiments.

1. Waves
I. Weinblum, Georg P.
II. Kendrick, Janet J., jt. auth.
III. Todd, M. Allison, jt. auth.
IV. Title: Wave effects produced by a thin body

David W. Taylor Model Basin. Rept. 840.
INVESTIGATION OF WAVE EFFECTS PRODUCED BY A THIN BODY - TMB MODEL 4125, by Georg P. Weinblum, Janet J. Kendrick, and M. Allison Todd. Washington, November 1952. ii, 14 p. incl. tables, figs., refs.
UNCLASSIFIED

A thin friction body is used to check experimentally Michell's wave resistance theory. The wave resistance experienced by the model and the wave profiles along the hull are calculated. These theoretical values are compared with the results of the experiments.

1. Waves
I. Weinblum, Georg P.
II. Kendrick, Janet J., jt. auth.
III. Todd, M. Allison, jt. auth.
IV. Title: Wave effects produced by a thin body

David W. Taylor Model Basin. Rept. 840.
INVESTIGATION OF WAVE EFFECTS PRODUCED BY A THIN BODY - TMB MODEL 4125, by Georg P. Weinblum, Janet J. Kendrick, and M. Allison Todd. Washington, November 1952. ii, 14 p. incl. tables, figs., refs.
UNCLASSIFIED

A thin friction body is used to check experimentally Michell's wave resistance theory. The wave resistance experienced by the model and the wave profiles along the hull are calculated. These theoretical values are compared with the results of the experiments.

1. Waves
I. Weinblum, Georg P.
II. Kendrick, Janet J., jt. auth.
III. Todd, M. Allison, jt. auth.
IV. Title: Wave effects produced by a thin body

David W. Taylor Model Basin. Rept. 840.
INVESTIGATION OF WAVE EFFECTS PRODUCED BY A THIN BODY - TMB MODEL 4125, by Georg P. Weinblum, Janet J. Kendrick, and M. Allison Todd. Washington, November 1952.
ii, 14 p. incl. tables, figs., refs.
UNCLASSIFIED

A thin friction body is used to check experimentally Michell's wave resistance theory. The wave resistance experienced by the model and the wave profiles along the hull are calculated. These theoretical values are compared with the results of the experiments.

1. Waves
I. Weinblum, Georg P.
II. Kendrick, Janet J., jt. auth.
III. Todd, M. Allison, jt. auth.
IV. Title: Wave effects produced by a thin body

David W. Taylor Model Basin. Rept. 840.
INVESTIGATION OF WAVE EFFECTS PRODUCED BY A THIN BODY - TMB MODEL 4125, by Georg P. Weinblum, Janet J. Kendrick, and M. Allison Todd. Washington, November 1952.
ii, 14 p. incl. tables, figs., refs.
UNCLASSIFIED

A thin friction body is used to check experimentally Michell's wave resistance theory. The wave resistance experienced by the model and the wave profiles along the hull are calculated. These theoretical values are compared with the results of the experiments.

1. Waves
I. Weinblum, Georg P.
II. Kendrick, Janet J., jt. auth.
III. Todd, M. Allison, jt. auth.
IV. Title: Wave effects produced by a thin body

David W. Taylor Model Basin. Rept. 840.
INVESTIGATION OF WAVE EFFECTS PRODUCED BY A THIN BODY - TMB MODEL 4125, by Georg P. Weinblum, Janet J. Kendrick, and M. Allison Todd. Washington, November 1952.
ii, 14 p. incl. tables, figs., refs.
UNCLASSIFIED

A thin friction body is used to check experimentally Michell's wave resistance theory. The wave resistance experienced by the model and the wave profiles along the hull are calculated. These theoretical values are compared with the results of the experiments.

1. Waves
I. Weinblum, Georg P.
II. Kendrick, Janet J., jt. auth.
III. Todd, M. Allison, jt. auth.
IV. Title: Wave effects produced by a thin body

David W. Taylor Model Basin. Rept. 840.
INVESTIGATION OF WAVE EFFECTS PRODUCED BY A THIN BODY - TMB MODEL 4125, by Georg P. Weinblum, Janet J. Kendrick, and M. Allison Todd. Washington, November 1952.
ii, 14 p. incl. tables, figs., refs.
UNCLASSIFIED

A thin friction body is used to check experimentally Michell's wave resistance theory. The wave resistance experienced by the model and the wave profiles along the hull are calculated. These theoretical values are compared with the results of the experiments.

1. Waves
I. Weinblum, Georg P.
II. Kendrick, Janet J., jt. auth.
III. Todd, M. Allison, jt. auth.
IV. Title: Wave effects produced by a thin body